Revista de Metalurgia
October-December 2021, 57 (4), e210
ISSN-L: 0034-8570
https://doi.org/10.3989/revmetalm.210

Analysis on surface integrity and sustainability assessment in electrical discharge machining of engineered Al-22%SiC metal matrix composite

Subhashree Naik[a], Sudhansu Ranjan Das[a,*], Debabrata Dhupal[a], Ajit Kumar Khatua[b]

[a] Department of Production Engineering, Veer Surendra Sai University of Technology, Burla 768018, Odisha, India
[b] Department of Mechanical Engineering, TempleCity Institute of Technology & Engineering, Khurda 752057, Odisha, India

(*Corresponding author: das.sudhansu83@gmail.com)

Submitted: 1 June 2021; Accepted: 26 November 2021; Available On-line: 30 December 2021

ABSTRACT. In view of the widespread applications of engineered metal matrix composites, particularly in automobile, electricity, aerospace industries; the achievement of the desired form is a really tough challenge. This research addresses electrical discharge machining (EDM) of engineered Al-22%SiC metal matrix composite (MMC) to analyze the surface roughness of the machined parts. A series of machining trials are performed under varied process conditions (flushing pressure, gap voltage, pulse-on-time, discharge current, pulse-off-time) obtained by Box-Behnken design. Additionally, this work addresses on desirability optimization methodology and predictive modelling for the minimization of machined surface quality employing the response surface methodology (RSM). Based on the motivational viewpoint of "Go green-Think green-Act green", a unique approach has been suggested for the economic analysis and the sustainability assessment to determine the overall machining cost per part and to justify the usefulness of vegetable oil as dielectric medium in the EDM process. According to this statistical analysis, the contribution of spark discharge current was identified as the leading factor in surface quality degradation. The estimated optimal surface roughness (Ra) value of 0.181 μm and the calculated overall machining cost per part of Rs. 245.9 (2.95 €) were preferred at pulse-on-time of 100 μs, gap voltage of 1 V, pulse-off-time of 30 μs, discharge current of 4 A and flushing pressure of 0.056 MPa, which indicates that it is techno-economically viable. The vegetable oil considered as dielectric fluid is biodegradable, environmentally safe and, thus, contributes to having a sustainable production. The Al-SiC MMC machining data would be beneficial to the industry.

KEYWORDS: Al-22%SiC MMC; Cost estimation; EDM; RSM; Surface finish; Sustainability

Citation/Citar como: Naik, S.; Das S.R.; Dhupal, D.; Khatua, A.K. (2021). "Analysis on surface integrity and sustainability assessment in electrical discharge machining of engineered Al-22%SiC metal matrix composite". *Rev. Metal.* 57(4): e210. https://doi.org/10.3989/revmetalm.210

RESUMEN: *Análisis de la integridad de la superficie y evaluación de la sostenibilidad en el mecanizado por electroerosión de un material compuesto de matriz metálica ingenieril Al-22% SiC.* En vista de las amplias aplicaciones que tienen los materiales compuestos ingenieriles de matriz metálica, particularmente en las industrias automotriz, eléctrica y aeroespacial, dar forma a estos materiales es un desafío realmente difícil. Esta investigación aborda el mecanizado por electroerosión de un material compuesto de matriz metálica Al-22% SiC para analizar la rugosidad de la superficie de las piezas mecanizadas. Se realizan una serie de pruebas de mecanizado en diversas condiciones de procesado (presión de chorro, voltaje, tiempo de activación del pulso, corriente de descarga, tiempo de desactivación del pulso) obtenido por un diseño Box-Behnken. Adicionalmente, este trabajo aborda la metodología de optimización deseada y modelado predictivo para la minimización de la calidad de la superficie mecanizada empleando la metodología de superficie de respuesta. Basado en el punto de vista motivacional de "Sea verde-piense en verde-actúe en verde", se ha sugerido un enfoque único para el análisis económico y la evaluación de sostenibilidad para determinar el costo total de mecanizado por pieza y para justificar la utilidad del aceite vegetal como medio dieléctrico en el proceso de electroerosión. De acuerdo con este análisis estadístico, la contribución de la corriente de descarga de chispa se identificó como el factor principal en la degradación de la calidad de la superficie. El valor de rugosidad superficial óptima estimado (Ra) de 0,181 μm y el coste total de mecanizado calculado por pieza de Rs. 245,9 (2,95 €) se prefirieron con un tiempo de activación del pulso de 100 μs, voltaje de 1 V, tiempo de desactivación de pulso de 30 μs, corriente de descarga de 4 A y presión de lavado de 0,056 MPa, lo que indica que es tecno-económicamente viable. El aceite vegetal considerado como fluido dieléctrico es biodegradable, ambientalmente seguro y, por tanto, contribuye a tener una producción sostenible. Los datos de mecanizado de este material compuesto Al-SiC serían beneficiosos para la industria.

PALABRAS CLAVE: Acabado superficial; Electroerosión; Estimación de costes; Material compuesto de matriz metálica Al-22%SiC; Metodología de superficie de respuesta; Sostenibilidad.

ORCID ID: Subhashree Naik (https://orcid.org/0000-0002-8456-4043); Sudhansu Ranjan Das (https://orcid.org/0000-0003-2723-4459); Debabrata Dhupal (https://orcid.org/0000-0001-9428-294X); Ajit Kumar Khatua (https://orcid.org/0000-0001-7278-3743)

1. INTRODUCTION

One of the main issues for manufacturing with today's technology is ensuring the specified product in an effective and the most economical way. In the present scenario, MMCs have expanded their different industrial applications to attain high levels of efficiency in view of their unique characteristics (high specific strength, excellent resistance to thermal distortion, wear & corrosion, and light-weight than traditional materials) (Mohan *et al.*, 2004). From a commercial production point-of-view, the conventional machining processes are incompetent in terms of machining of aluminum-based MMC within an acceptable tolerance limit. In fact, these MMCs can often be difficult-to-machine due to the strength and hardness of the reinforcement. Owing to its highly flexible manufacturing versatility, electrical discharge machining (EDM) is the most common non-conventional machining method applied for the removal of extremely hard materials effectively, with complex-integrate shape, in the manufacturing for miniaturization of given developments applicable to aerospace, defense, automobile, electronic, and nuclear industries. It employs a thermoelectric source of energy to machine electrically conductive parts irrespective of hardness. The process of material removal by controlled erosion via a series of pulsating electric sparks causes melting and vaporization of metal to produce an almost a stress-free finished surface.

Despite everything, in view of the complex-dynamic performance of the EDM mechanism and its strong links with the different variables, achieving the high production efficiency from a technologically-economic perspective is important. Various factors that influence the cutting phenomena during EDM are: dielectric flushes (dielectric fluids & its flushing pressure), electrode & workpiece materials, electro-spark variables (voltage, discharge current, pulse duration, frequency), and others. A proper machining criterion to achieve an optimum process efficiency is still a difficult task, as modern technical approaches enable significant progress in decision making. Experimental methodologies, modeling, and optimization techniques play a critical role in such situations. For this reason, researchers have approached various statistical (Yildiz *et al.*, 2012; Sivam *et al.*, 2013; Uyyala *et al.*, 2014; Gohil and Puri, 2016; Singh *et al.*, 2019; Chaudhury and Samantaray, 2021) and computational (Bharathi Raja *et al.*, 2013; Garcia Rojas *et al.*, 2013; Cakir *et al.*, 2013; Mohanty *et al.*, 2017; Sahu *et al.*, 2020; Ramesh and Jenarthanan, 2021) methods in their works for predictive modelling (Puertas and Perez, 2003; Keskin *et al.*, 2005; Markopoulos *et al.*, 2008; Gao *et al.*, 2008; Chattopadhyay *et al.*, 2009; Pradhan *et al.*, 2009; Shabgard *et al.*, 2009; Gopalakannan and Senthilvelan, 2013; Yadav and Yadava, 2014; Kumar *et al.*, 2014; Majumder, 2014; Talla *et al.*, 2015; Selvarajan *et al.*, 2017; Belloufi *et al.*, 2020), parametric optimization (Singh, 2012; Bharti *et al.*, 2012; Tang and Guo, 2013; Tang and Du, 2014; Prabhu *et al.*, 2013; Tzeng and Chen, 2013; Reddy *et al.*, 2014; Singh *et al.*, 2015; Marichamy *et al.*, 2016; Prakash *et al.*, 2016; Kumar *et al.*, 2017; Rahul *et al.*, 2017; Singh and Sharma, 2017; Senthil Kumar and Suresh, 2019; Hanif *et al.*, 2019; Jagadish *et al.*, 2021) in EDM process with a view to control and to improve the surface finish of machined parts without compromising the product quality.

From the open literatures, none of these studies have explored the machining of Al-22%SiC based MMC via EDM. Although numerous studies have been executed in recent years and focused on their assessment for achieving high machining efficiency in EDM. In view of machined surface morphology was not intensively highlighted in absence of MRR, electrode wear rate. In the true experience of authors, yet no literature has reported on the cost assessment for EDM of Al-SiC MMC, which is still a matter of concern from an economical point of view. Regarding the existing literature, the knowledge related to the assessment of sustainability performance of EDM using vegetable oil as dielectric medium is not available up to date, which opens up a window of research to establish the process based on the motivational viewpoint of "Go green-Think green-Act green". Though, literatures related to usage of a response surface methodology for the optimization and modelling in EDM are available in large numbers, unfortunately there has been no systematic study. In perspective to fill the research gaps as stated above, the following objectives have been set for the present work: (i) Investigation on surface quality and economic cost assessment during EDM of newly engineered Al-22%SiC MMC under the influence of cutting parameters (flushing pressure, gap voltage, discharge current, pulse-off-time, pulse-on-time); (ii) Predictive modelling and parametric optimization for minimization of surface roughness in EDM by response surface methodology; (iii) Comparative sustainability evaluation between kerosene and vegetable oil as dielectric mediums for safer and cleaner approach of an environmentally friendly manufacturing.

All of these contributions provide worthwhile research, add to the uniqueness of the present study, and establish the improvement in favor of sustainable machining.

2. EXPERIMENTAL SETUP AND PROCEDURE

2.1. Materials

A newly engineered Al-22%SiC metal matrix composite produced in the form of circular plate

Figure 1. Preparation and machining of Al-22%SiC MMC.

(size: 65 mm diameter and 5 mm thickness) is chosen as work material. Stir casting process was adopted for the production of Al-SiC metal matrix composites. The parameters controlling the quality of the casting are heating temperature, duration of heating, stirring time and the position of the stirrer in the molten mixture. Scraps of aluminum of around 1 kg were put in the crucible. Then the crucible was placed in an electrically heated furnace. The crucible was heated to 700 ºC for 60 minutes. Flux was added in the molten mixture in the crucible. Argon gas was passed in the mixture to protect it from coming in contact with the environment. Dross was taken out from the mixture by a perforated flat spoon. The temperature of the mixture was kept at 700 ºC for 15 minutes. 22 wt.-% SiC particles of size 300 to 400 µm, preheated to 600 ºC, were added in the molten mixture. A three-blade impeller was mounted at 120° × 45° to stir the melt mixture and uniformly mix the reinforcements. The stirrer was moved up and down in the molten mixture during stirring. Stirring was continued for 10 minutes to have an even distribution of SiC particles in the mixture. The diffusion of aluminum silicon carbide occurs in three stages; aluminium-aluminium (Al-Al), aluminum-silicon carbide (Al-SiC), silicon carbide-silicon carbide (SiC-SiC). The grain growth rate of SiC-SiC is much faster than the other two combinations, which, if not controlled, might dominate the final grain structure of the material. In order not to let this happen, a small amount of around 0.1% NaCl powder was added just before casting. Castings in the shape of cylindrical rods (diameter 65 mm) were obtained by putting the molten metal into a cast iron permanent mould. Thereafter, the cylindrical rod was cut by a wire-EDM into six pieces with these pieces having a thickness of 5 mm. Grinding and polishing at different grades of particles was carried out to prepare the samples for microstructural examination and for the present experimental purpose. Figure 1 pictorially illustrates the preparation and machining of Al-22%SiC MMC. Figure 2 depicts SEM micrograph embedded with EDS map of Al-22%SiC MMC. It is clearly seen from the micrograph that the uniform distribution of the particles was found where no reactions were observed between Al and SiC particles due to proper mixing and preheating of the particles before pouring them into the molten pool. It confirms the presence of main constituents like C, O, Mg, Al, and Si in the spectroscopy analysis as indicated by Fig. 2b.

Domestically available ecofriendly, bio-degradable vegetable sunflower oil is used as a dielectric medium during EDM. The properties of the sunflower oil are presented in Table 1. Brass rod (size: diameter of 9 mm) is employed as the electrode material. Since EDM is a thermal process, new and identical tools were employed for each experimental run so that the effects of tool wear on the machining performance could be avoided. The SEM & optical micrographs and EDX analysis of the tool electrode before machining are presented in Fig. 3.

2.2. Experimental setup

To perform machining trials, a high accuracy electric discharge machine (ECOWIN, MIC 432CS) was employed. During the experimental trials at each parameter settings, the evaluation of surface finish of machined component, in terms of the arithmetic average roughness (Ra), was determined by a Surftest SJ-210 Mitutoyo roughness tester with a cut-off length of 0.8 mm and evaluation length of 4 mm. In order to facilitate the surface roughness measurement with the highest precision possible, the machined components were fixed in a miniature

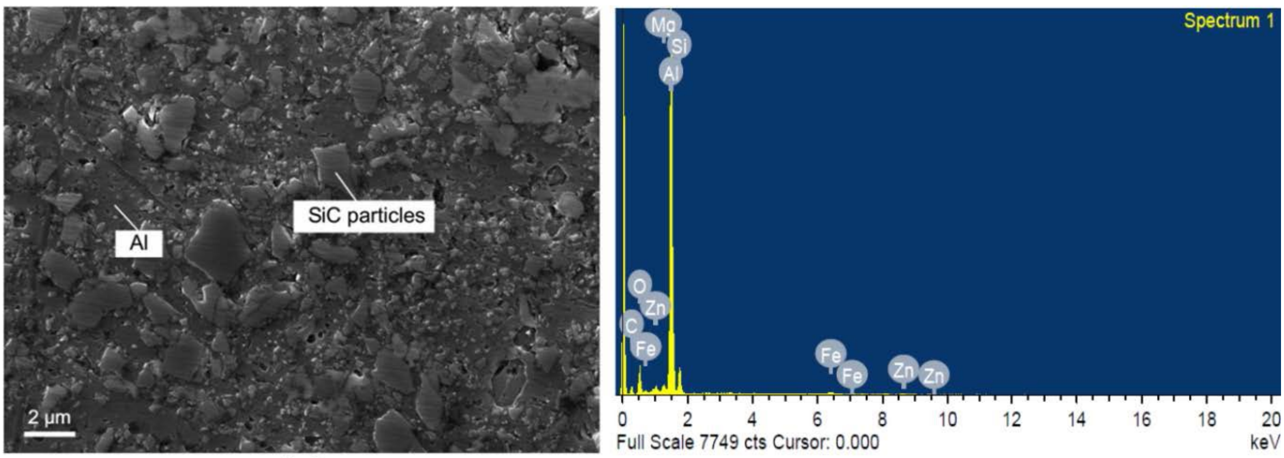

(a) (b)

Figure 2. (a) SEM micrograph and (b) EDX spectrum of Al-22%SiC MMC microstructure.

Table 1. Characteristics of vegetable sunflower oil (Garcia Rojas *et al.*, 2013).

Properties	Value
Density	919 $kg \cdot m^{-3}$ at 20 °C
Dynamic viscosity	6.3×10^{-5} $m^2 \cdot s^{-1}$ at 20 °C
Flash point	325 °C
Thermal conductivity	0.162 $W \cdot m\text{-}K^{-1}$ at 20 °C
Heat capacity	2.124 $J \cdot g\text{-}K^{-1}$ at 20 °C
Calorific value	39.18 $kJ \cdot kg^{-1}$
Dielectric constant	2.95 at 25 °C

vice and the stylus probe of roughness tester was then inserted into the hole to measure the sidewall surface finish of hole. The measurements were repeated three times at three reference lines equally positioned at 120° of the sidewall surfaces of the cylindrical shaped machined holes and only the averaged value was considered under each machining condition (Fig. 4). Once the surface roughness was measured, with the specific goal to study the various surface integrity aspects, samples were cut from the machined surface with the help of wire-electrical discharge machine (WEDM). Prior to testing, the cold-mounted specimens were polished with different grit size of waterproof SiC papers of grade (P600, P800, P1000, P1200 & P1500). Finally, the specimen surface has been polished by velvet cloth with diamond paste of 1 μm size and last by Hifin fluid. Next, the polished surface has been chemically etched with 2% Nital (a solution of ethyl alcohol and nitric acid) for 20 seconds immersion. The specimen prepared by the above mentioned stan-

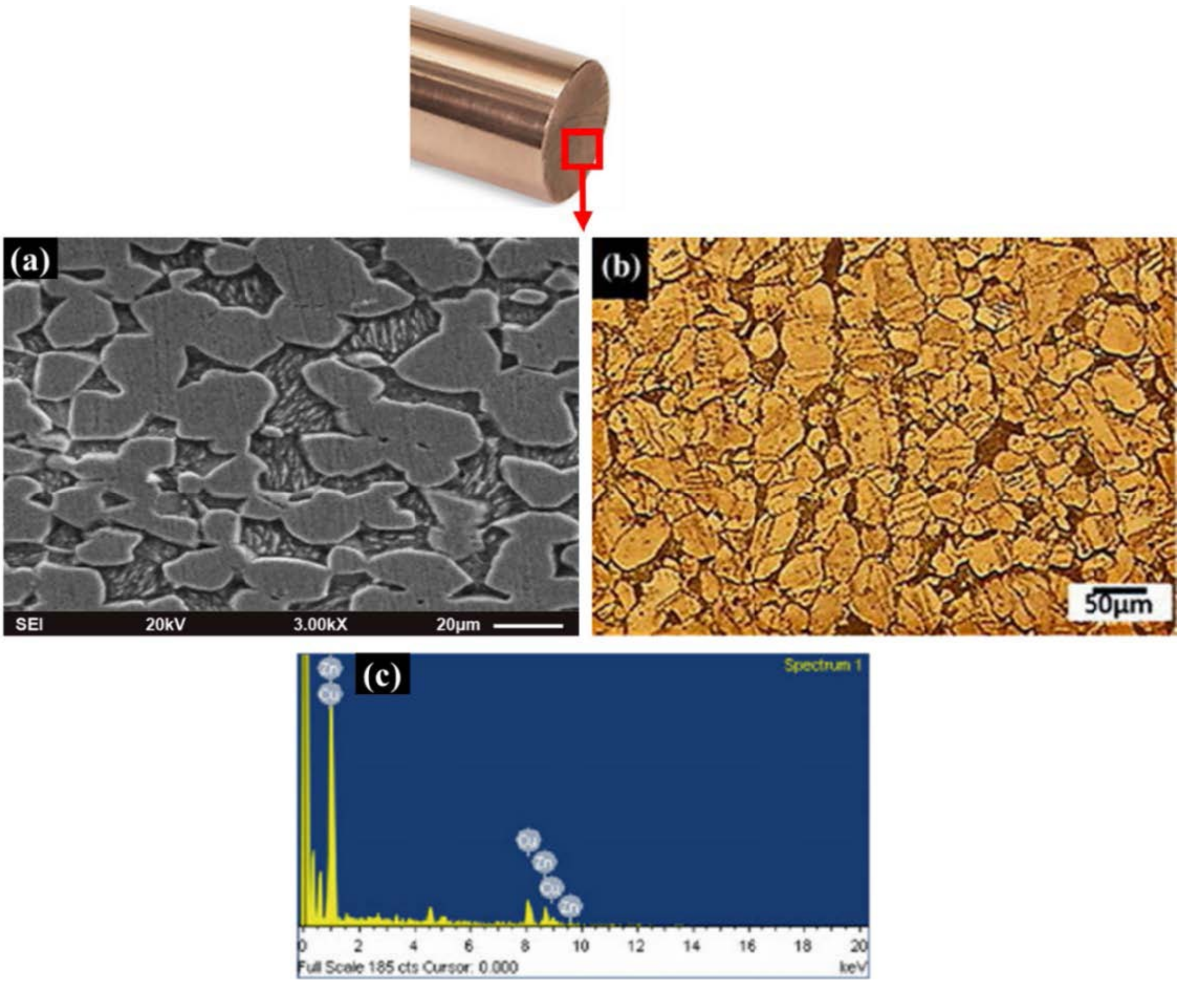

Figure 3. (a) SEM image, (b) optical micrograph and (c) EDX analysis brass electrode before machining.

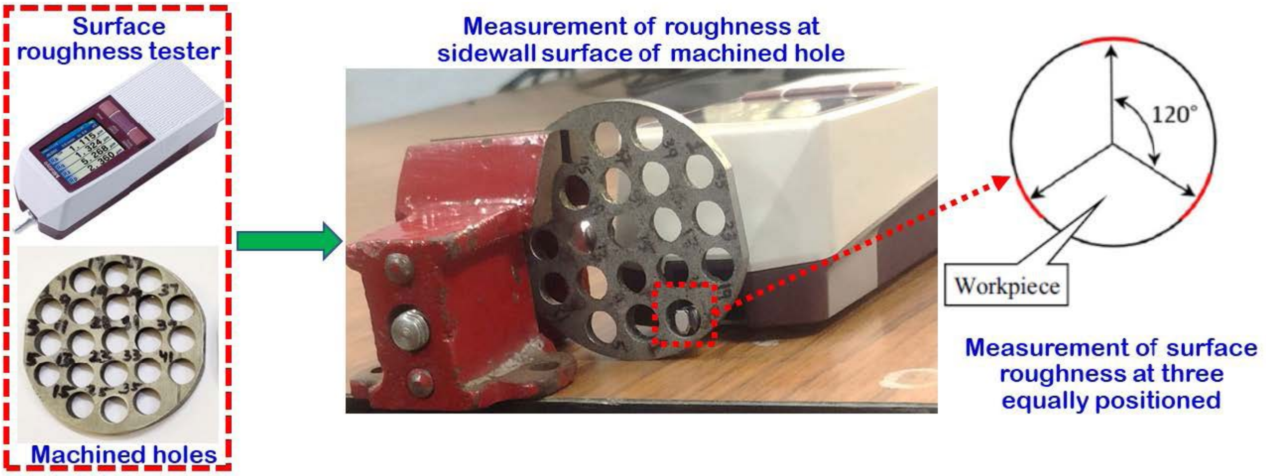

Figure 4. Schematic description of surface roughness measurement.

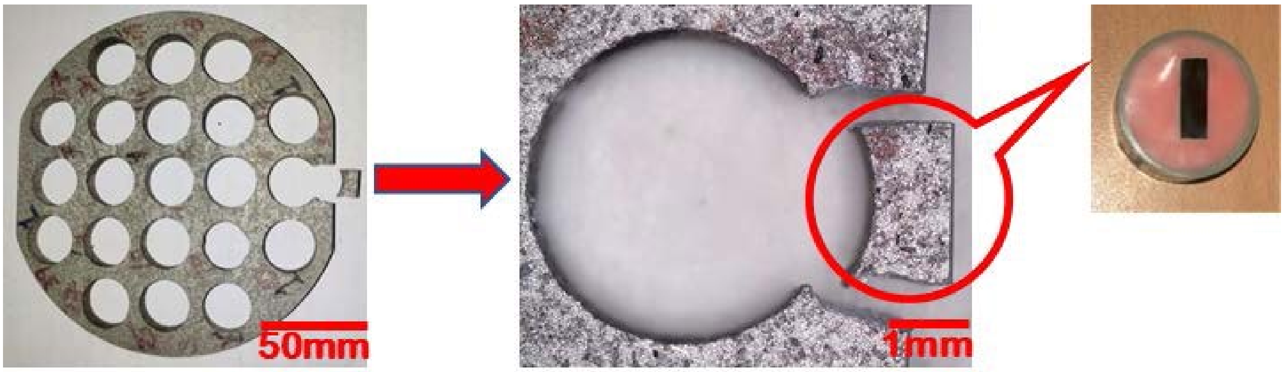

Figure 5. Cold mounted specimen used for white layer observations.

dard metallographic techniques were used in order to reveal the white layer formation on the machined surface. Figure 5 depicts snapshot of cold-mounted specimen. Coordinate measuring machine (ZEISS MC850) embedded with a stylus was employed for measurement of overcut (OC) of machined hole. Additionally, a scanning electron microscope (JEOL JSM-6480LV) has been employed for the morphological study (white layer formation, surface crack intensity) of the machined surface.

The number of machining trial were designated according to Box-Behnken design, considered based on RSM which is associated with five control factors each of having three levels namely discharge current (5, 10, 15 A), gap voltage (1, 1.5, 2 V), pulse-on-time (100, 200, 300 µs), pulse-off-time (10, 20, 30 µs) and flushing pressure (0.020, 0.039, 0.059 MPa). The remaining process variables are kept constant as shown in Table 2. The considered input parameters have predominant impacts on various output criteria of the EDM process, as the discharge current and pulse-on-time can influence the plasma channel and plasma diameter. Thus, the temperature distribution along and into the workpiece material will differ significantly, and would have an impact on the surface roughness. The flushing pressure prevents the accumulation of erosion products and flushes the erosion pockets in between the gap of electrode and the work surfaces. Gap voltage provides the flushing conditions and helps to stabilize the machining to achieve the desired depth. The selection of different levels of control parameters are considered on the basis of extensive literature surveys that have reported these parameters to be most influential for the surface roughness. Moreover, the range of process parameters setting have been selected after performing some pilot experi-

Table 2. Parameters kept at constant values.

Parameters	Unit	Value
Duty cycle	%	85
Polarity	--	Workpiece (positive)
Machining depth	mm	5
Spark gap	µm	50

Table 3. Experimental plan layout and results.

Test. Nº	Machining process parameters					Machining response
	DC (A)	GV (V)	Ton (µs)	Toff (µs)	FP (MPa)	Ra (µm)
1	5	1.0	200	20	0.039	0.176
2	15	1.0	200	20	0.039	0.700
3	5	2.0	200	20	0.039	0.204
4	15	2.0	200	20	0.039	0.353
5	10	1.5	100	10	0.039	0.418
6	10	1.5	300	10	0.039	0.388
7	10	1.5	100	30	0.039	0.400
8	10	1.5	300	30	0.039	0.717
9	10	1.0	200	20	0.020	0.454
10	10	2.0	200	20	0.020	0.402
11	10	1.0	200	20	0.059	0.462
12	10	2.0	200	20	0.059	0.420
13	5	1.5	100	20	0.039	0.186
14	15	1.5	100	20	0.039	0.623
15	5	1.5	300	20	0.039	0.212
16	15	1.5	300	20	0.039	0.432
17	10	1.5	200	10	0.020	0.413
18	10	1.5	200	30	0.020	0.427
19	10	1.5	200	10	0.059	0.567
20	10	1.5	200	30	0.059	0.758
21	10	1.0	100	20	0.039	0.380
22	10	2.0	100	20	0.039	0.344
23	10	1.0	300	20	0.039	0.457
24	10	2.0	300	20	0.039	0.385
25	5	1.5	200	10	0.039	0.221
26	15	1.5	200	10	0.039	0.292
27	5	1.5	200	30	0.039	0.171
28	15	1.5	200	30	0.039	0.754
29	10	1.5	100	20	0.020	0.475
30	10	1.5	300	20	0.020	0.391
31	10	1.5	100	20	0.059	0.428
32	10	1.5	300	20	0.059	0.749
33	5	1.5	200	20	0.020	0.391
34	15	1.5	200	20	0.020	0.431
35	5	1.5	200	20	0.059	0.213
36	15	1.5	200	20	0.059	0.782
37	10	1.0	200	10	0.039	0.450
38	10	2.0	200	10	0.039	0.361
39	10	1.0	200	30	0.039	0.416
40	10	2.0	200	30	0.039	0.411
41	10	1.5	200	20	0.039	0.452
42	10	1.5	200	20	0.039	0.522
43	10	1.5	200	20	0.039	0.438
44	10	1.5	200	20	0.039	0.395
45	10	1.5	200	20	0.039	0.382
46	10	1.5	200	20	0.039	0.372

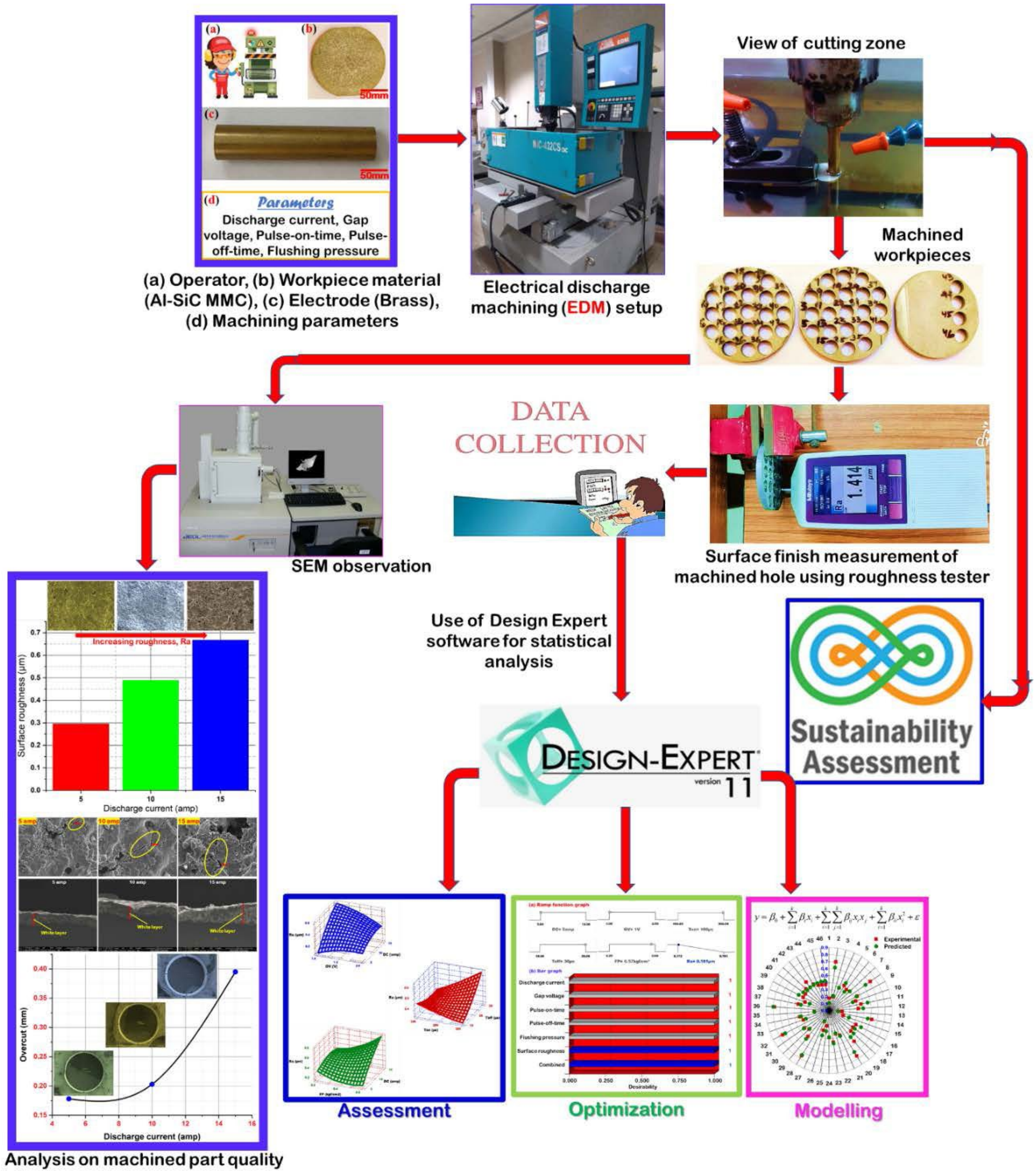

FIGURE 6. Schematic of machining setup and procedure followed for the experimental investigation.

ments and also by inspecting the workpiece for a through hole of acceptable quality. Experimental layouts results consisting of forty-six runs are presented in Table 3. For a through hole, each test was carried out with 5 mm of machining depth, which resulted the different cutting times for every parameter setting, in accordance of DOE. Figure 6 pictorially represents the schematic layout of the procedure followed for the machining setup and experimental investigations.

3. RESULTS AND DISCUSSION

3.1. Predictive model development using RSM

The present study exploited the technique of RSM to establish the second order empirical model for the relationship among the machining variables (GV, DC, T_{on}, T_{off}, FP) and the technological response (Ra) using Design Expert 11.0 software. Response surface methodology constitutes a group of statistical techniques that enables the experimental design for statistical model development, operating variable assessment, and the estimation of the values of operating variables that will maximize the desirable responses. Using this RSM model of the response function in this study was not only to investigate over the entire factor space, but also to locate the targeted region desired where the response approaches its optimum or near optimal value. The established regression model of dependent variables (here, Ra) is represented by Eq. (1).

$$\begin{aligned} R_a = {} & 1.025 + 0.0545DC + 0.73GV - 0.00251T_{on} - 0.0622T_{off} - 4.002FP - 0.002412DC^2 \\ & - 0.1632GV^2 + 0.000001T_{on}^2 + 0.00025T_{off}^2 + 1.872FP^2 - 0.0375DC * GV \\ & - 0.000108DC * T_{on} + 0.00256DC * T_{off} + 0.1322DC * FP - 0.00018GV * T_{on} \\ & + 0.0042GV * T_{off} + 0.025GV * FP + 0.000087T_{on} * T_{off} + 0.00506T_{on} * FP \\ & + 0.0221T_{off} * FP \end{aligned} \tag{1}$$

$R^2 = 88.97\%$, $R^2(adj.) = 80.14\%$

It is a common procedure in ANOVA to conduct statistical significance of model and independent variables for the performance measures at certain confidence level. In the analysis, the sum-of-squares (SS), mean-of-squares (MS) and variance are calculated. F-value as well as P-value at 95% CI level decides the significant factors affecting the response and the last column of the ANOVA table represents the percentage contribution of each parameter while machining. As the experimental results were modelled at 95% confidence level, a parameter and regression model are considered to be significant if the statistical index P-value is below 0.05. Meanwhile, the calculated F-value larger than Fisher's (F) standard value, shows a noticeable effect on the output. Table 2 illustrates the ANOVA results of the model developed for the surface roughness, which clearly indicates the excellent significance of the model. Moreover, from the Table 4, it is apparent that the most influencing parameter on Ra is the discharge current with the highest percent contribution (38.21%), because its P-value is more than 0.05, which clearly agrees with the previous studies (Mohanty *et al.*, 2014; Raza *et al.*, 2018; Naik *et al.*, 2020). In the similar context, ANOVA results revealed GV, Toff, FP, FP*FP, DC*DC, Ton*Toff DC*GV, DC*FP, DC*Toff, and Ton*FP are the significant terms at 95% CI level since their F-values are larger than F table values and P-value below 0.05. The factor pulse-on-time and interaction terms (GV*FP, Toff*Toff, GV*GV, DC*Ton, Ton*Ton, GV*Ton, GV*Toff, Toff*FP) are inconsiderable due to their undesirable P-values.

Table 4. ANOVA result for predictive surface roughness model.

Source	F-value	P-value	Contr., %
Model	10.08	<0.00001	88.97
Linear	23.72	<0.00001	52.34
DC	86.57	<0.00001	38.21
GV	4.87	0.037	2.15
Ton	2.93	0.990	1.29
Toff	11.47	0.002	5.06
FP	12.75	0.001	5.63
Square	5.74	0.001	12.68
DC*DC	6.54	0.017	4.74
GV*GV	2.99	0.096	3.36
Ton* Ton	0.18	0.674	0.12
Toff*Toff	1.12	0.300	0.02
FP*FP	10.08	0.004	4.45
2-Way Interaction	5.43	<0.00001	23.95
DC*GV	7.24	0.013	3.2
DC*Ton	2.43	0.132	1.07
DC*Toff	13.5	0.001	5.96
DC*FP	14.41	0.001	6.36
GV*Ton	0.07	0.798	0.03
GV*Toff	0.36	0.552	0.16
GV*FP	0.01	0.943	0.00
Ton*Toff	6.20	0.020	2.74
Ton*FP	8.45	0.008	3.73
Toff*FP	1.61	0.216	0.71
Error			11.03
Lack-of-Fit	1.66	0.300	9.59
Pure Error			1.44
Total			100

Table 5. Descriptive statistics of error comparison for surface roughness.

Run Nº	1	2	3	4	5	6	7	8	9	10	11	12	13	14	15	16	17	18	19	20	21	22	23
M*	0.176	0.7	0.204	0.353	0.418	0.388	0.4	0.717	0.454	0.402	0.462	0.42	0.186	0.623	0.212	0.432	0.413	0.427	0.567	0.758	0.38	0.344	0.457
P**	0.191	0.643	0.219	0.346	0.460	0.346	0.421	0.657	0.483	0.368	0.489	0.447	0.210	0.563	0.239	0.494	0.450	0.479	0.486	0.692	0.396	0.361	0.483
Error (%)	8.52	8.14	7.35	2.09	9.99	10.85	5.36	8.31	6.39	8.51	5.84	6.47	13.15	9.62	12.54	14.40	8.89	12.23	14.36	8.69	4.13	4.94	5.76
Run Nº	**24**	**25**	**26**	**27**	**28**	**29**	**30**	**31**	**32**	**33**	**34**	**35**	**36**	**37**	**38**	**39**	**40**	**41**	**42**	**43**	**44**	**45**	**46**
M*	0.385	0.221	0.292	0.171	0.754	0.475	0.391	0.428	0.749	0.391	0.431	0.213	0.782	0.45	0.361	0.416	0.411	0.452	0.522	0.438	0.395	0.382	0.372
P**	0.410	0.248	0.327	0.192	0.789	0.521	0.423	0.453	0.705	0.349	0.409	0.240	0.813	0.491	0.393	0.457	0.451	0.427	0.427	0.427	0.427	0.427	0.427
Error (%)	6.49	12.42	11.84	12.28	4.64	9.68	8.18	5.81	5.87	10.64	5.09	12.68	3.96	9.21	8.74	9.96	9.63	5.57	18.23	2.55	8.06	11.74	14.74

* Measured-Ra, ** Predicted-Ra

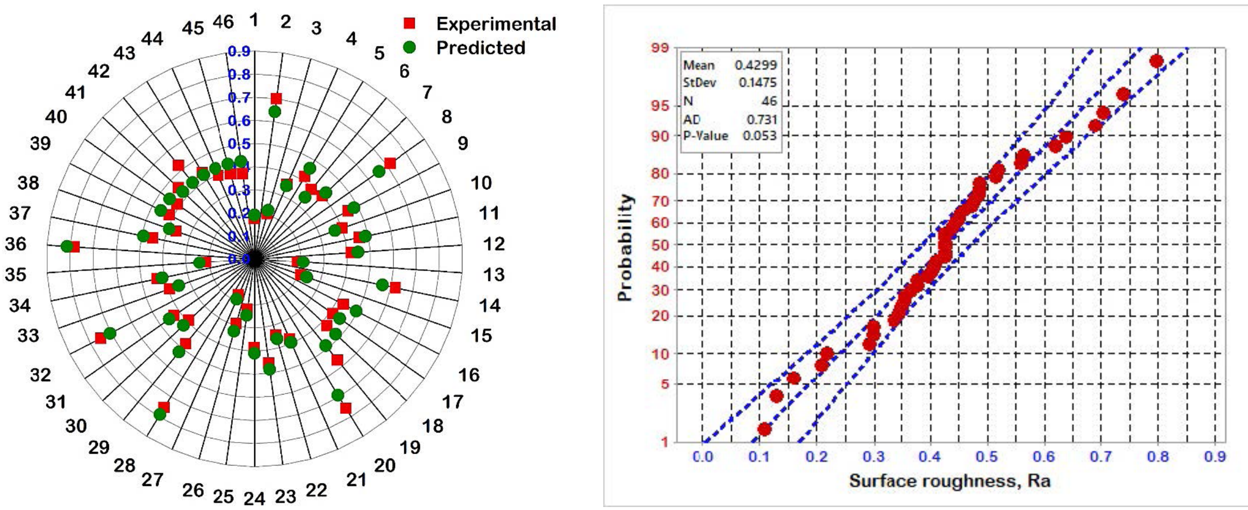

(a) (b)

Figure 7. (a) Predictive ability plot, (b) Normal probability (%) plot for Ra.

Multiple diagnostic tests including adequacy, efficacy and fitness-of-data are conducted for the suggested regression model to avoid reaching misleading conclusions. Generally, a higher R-squared (i.e., value close to 1) is desirable as it reveals a better fit for the model. The correlation coefficient of determination (R^2) value for surface roughness, as represented by quadratic regression model was estimated as 0.889%. From the model adequacy point-of-view, the R^2 values are justified in the present study since the proportion of variation in the response variable is highly associated with the independent variable. Also, it is evident from the Table 5 followed by Fig. 7a, an excellent resemblance between the measured and predicted values of Ra is achieved. Thus, it is concluded that the proposed model has high effectiveness with good predictability as the average error limited up to 9.43% which is very minimal. To undertake a better comparison of the predicted values attained via the regression equation with the experimental values, a normal probability plot is represented to show the positions of residuals on the linear curve as shown in Fig. 7b. The independent plotting reveals that almost all the residuals are given by nearness to the straight line which implies that the proposed model is in line up with the actual values. This establishes the reliability and integrity of the developed regression equation for predicting Ra. As far as Anderson-Darling test is concerned, the larger P-value (0.053) indicates that null-hypothesis criteria is accepted for a goodness to fit-of-data. In general, the developed predictive model for Ra using RSM suggested less deviation from the actual values resulting to the appropriateness of the model.

3.2. Surface roughness analysis

The influence of machining parameters on the surface roughness, R_a was examined by employing a three-dimensional surface response plot. It is evident from Fig. 8a that EDM with increasing discharge current degrades surface finish for the most part which may be because of increased current density and spark energy, which clearly agrees with the previous studies (Muthuramalingam and Mohan, 2013; Rahul *et al.*, 2019; Sahu and Datta, 2019). Moreover, this outcome is attributed to development of uneven deeper-larger crater marks on the surface of the machined part (due to increased MRR) at higher discharge currents. Figure 9 displays the SEM image and states the status of the poor machined surface with regard to crater marks (as a result of multifaceted interaction between dielectric flushing, debris, and continuous discharge spark), globular debris (in view of cold welding effects and cohesion of molten material and irregular flushing of dielectric fluid within gap), micro-cracks (based on induced internal residual stress over the tensile strength of work material resulting from prompt heating and cooling), micro-voids (attributed to evolved gas during spark erosion process), and micro-pores (as a consequence of low fracture toughness & thermal shock resistance of MMC). Based on certain EDM operation conditions (GV= 2 V; T_{on}= 200 µs; T_{off}= 20 µs; FP= 0.020 MPa), at high peak current, the discharge energy resulted in considerable melting and vaporization of MMC material that enhances the formation of irregularities on the machined surface. Such effects were better explained in Fig. 10. This figure reflects the SEM observations on the machined surfaces using different discharge currents. The micrographs explain the various surface defects at high temperature based on the energy propagation from the conducting elements that let the discharge current penetrate. Higher discharge energy thus hinders the surface integrity and compromises its applicability in a substantial way. From the 3D response graph for the surface roughness (Fig. 8b), it is noted that Ra is increasing with the increase in pulse-on-time. The reason for that is the availability of energy for material removal for a specified period is participated with a smaller extent by a substantial number of sparks at higher pulse-on time. Therefore, it exploits deep crater formation on the work surface and results in a rough surface. In addition, a lesser amount of metal is removed through smaller pulse-on-time, approaching an acceptable accuracy due to a moderate thermal damage to the machined component, developing improved surface finish. The forced circulation of the dielectric has been found to promote a significant improvement in the surface

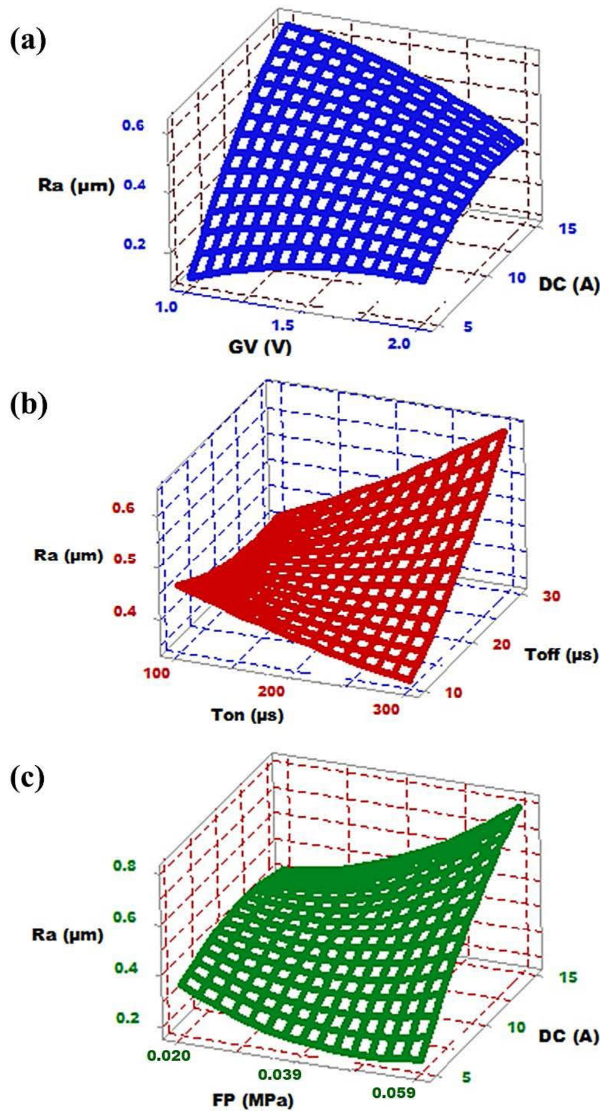

FIGURE 8. 3D response plot for surface roughness under the interaction effects of different process parameters: (a) GV-DC, (b) T_on-T_off, (c) DC-FP.

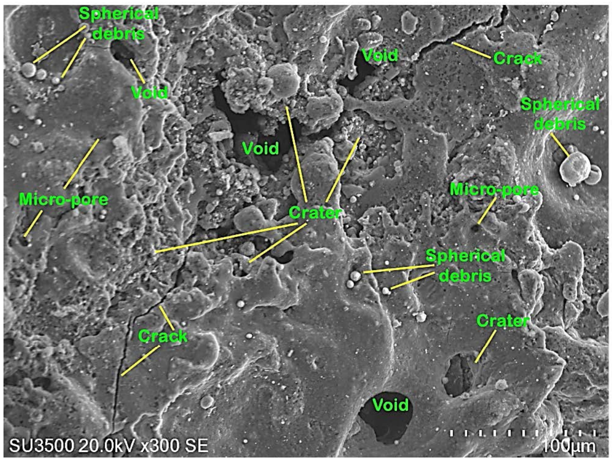

FIGURE 9. SEM micrograph of poor machined surface at GV= 1.5 V, DC= 15 A, Ton= 200 µs, FP= 0.059 MPa, Toff= 20 µs.

finish. From Fig. 8c, it was deduced that the surface roughness decreased with the flushing pressure as it avoids short-circuiting and stagnation of the flushing fluid during EDM.

The spark discharge allows the material to be removed (as represented by the debris particles) from the workpiece surface during the erosion process of EDM. The cutting efficiency greatly depends on the flushing of dielectric medium. The dielectric fluid is applied to evacuate the debris fragments and to dislodge the material away from work surface by its flushing pressure, which is under the stage of molten (or partially melted). Under a continuous machining process, a certain portion of molten metal is swept, while a residue material gets re-solidified (caused by quick evaporation of dielectric fluid) forming an extremely brittle white layer, which is quite different from the base material. Microscopic white layer images were captured under the scanning electron microscope. Figure 11 provides the SEM images of EDM Al-22%SiC MMC specimens using the following machining conditions: T_{off} = 20 µs; GV= 1 V; FP= 0.039 MPa; T*on*= 200 µs. The white layer thickness is proportional to the discharge current as revealed from the SEM observation. With the higher energy release in each spark, associated to an increased pulse energy, the amount of matrix material which is melted increases, resulting in a thicker recast layer as shown in Figure 11. Therefore, the factors governing the pulse energy, that is, pulse-on-time and peak current, are crucial for the severity of the induced residual stresses and crack formation. Kumar *et al.* (2020) reported that the presence of ceramic particles in the work material and variation of spark energy had produced a nonuniformity in the recast layer. The recast layer is noticed to be fine grained and hard.

The prompt heating and cooling of the machined surfaces during EDM causes inconsistent heat flow and metallurgical alterations. Thus, enormous residual stresses are developed and these are responsible for deteriorating the surface integrity and functionality of the machined parts. According to Ekmekci (2007), EDM operation often promotes an inhomogeneous heat flow and metallurgical transformations or plastic deformation, which is basically an inhomogeneous local phenomenon. These produces residual stress generated within the machined specimen. If the residual stress exceeds the maximum tensile strength of the machined surface, cracking occurs (Sahu *et al.*, 2018). Sometimes the deepness of the white layer penetrates them deeper and continues into the parent material. Increasing discharge energy forms unnecessary conducting paths between the tool electrode and workpiece that creates surface micro-cracks (Sahu *et al.*, 2018). Hence, intense heat flow at the vicinity of surface being machined, yielded higher crack

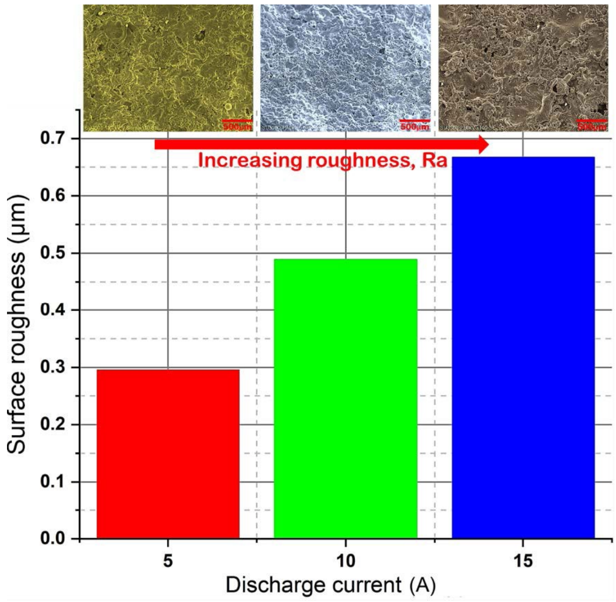

Figure 10. Effect of the discharge peak current on surface finish of machined parts at Ton= 200 µs; GV= 2 V; FP= 0.02 MPa; Toff= 20 µs.

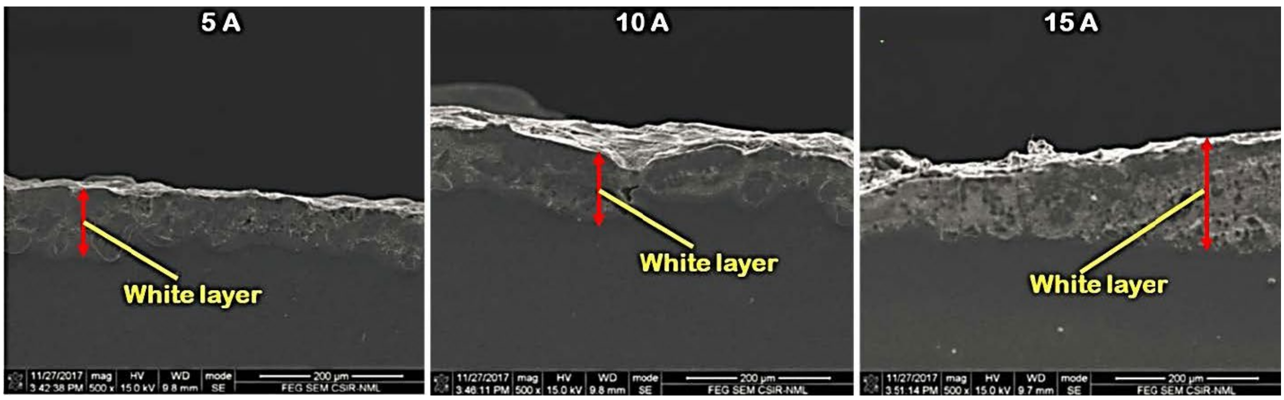

Figure 11. White layer thickness of observed in the machined surfaces under varied discharge currents at T_{on}= 200 µs; GV= 1 V; FP= 0.039 MPa; T_{off}= 20 µs.

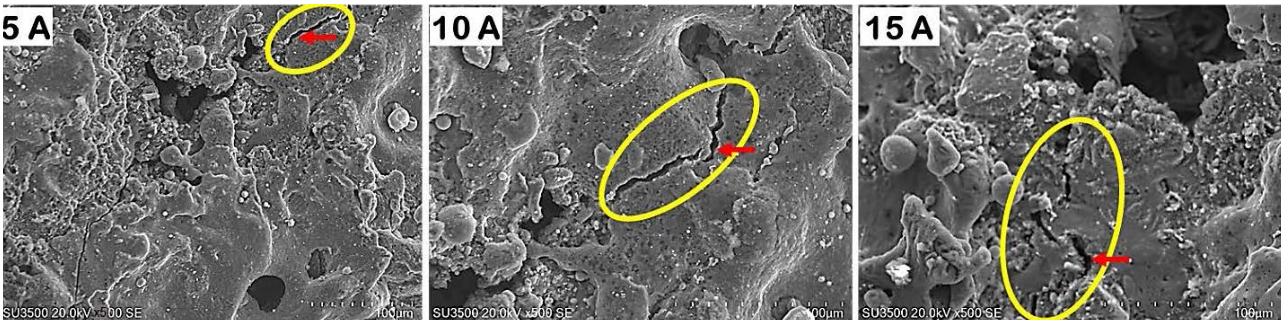

Figure 12. Surface cracking observed on the machined work surfaces of Al-22%SiC MMC obtained under the influence of various discharge currents.

intensity which is depicted in Fig. 12. This figure shows trends of increasing crack widths at higher discharge current. The explanation for increased crack width has been explained well by Rahul *et al.* (2019). The influence of peak current contributes to increase the discharge energy per spark and, accordingly, transfers considerable thermal energy to the machined upper surface. In comparison to the subsurface, this leads to more material evaporation and, consequently, produces uneven dimensional deviations of holes, leading to a larger overcut (refer, Fig. 13). The selected cutting conditions enlisting maximum geometric shape deformation of hole occurs at FP= 0.039 MPa; T_{on}= 200 µs; T_{off}= 20 µs; GV= 1 V. Mohanty *et al.* (2014) reported that increasing the discharge energy per every individual spark, as well as cutting time along with cutting velocity, transfers more thermal energy to the workpiece surface. This results in more evaporation of material in comparison to the sub-surface and, in turn, it increases the radial overcut caused by side spark erosion at the hole wall surface.

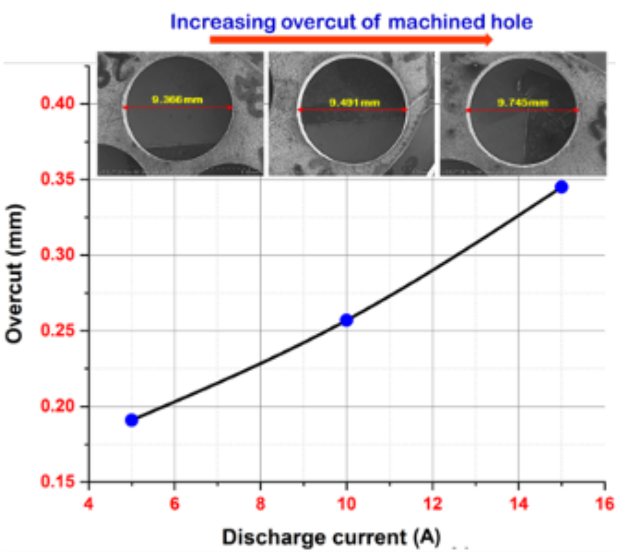

Figure 13. Dimensional deviation of the machined hole quality under varied discharge current.

3.3. Optimization of surface roughness using RSM

Recently, one of the best suitable techniques of optimization for mono and multi-objective and multiple responses in metal cutting processes is the desirability function analysis. This is based on multi-criteria decision making. Desirability is an objective function that translates each response in the scale ranging from zero outside of the limits to one at the goal. The variables result in an undesirable response if the value is 0, while a value of 1 is related to the best performance (i.e., highly desirable) for the studied variables. After the desirability functions are established for each different response variables, depending on its objectives, an overall desirability function is defined, which is obtained by combining the geometric mean of individual desirability functions. Once the overall desirability is defined, it can be used for optimal solution of predictors or responses. The Present work deals with the desirability optimization methodology for the minimization of the surface roughness of machined parts, Ra. Such task for the predicting of the optimal solution to the response (OC) was obtained using the standard statistical software package *Design Expert 11*. For solving the optimization problem, the individual desirability functions for the abovementioned output is stated as (Dash *et al.*, 2020);

$$d_i = \begin{cases} 1 & if\ y_i \le l_i \\ \left[\frac{u_i - y_i}{u_i - l_i}\right] & if\ l_i \le y_i \le u_i \\ 0 & if\ \ y_i \ge u_i \end{cases} \tag{2}$$

whereas, the overall desirability can be expressed as,

$$D = \left(\prod_{i=1}^{N} d_i\right) \tag{3}$$

and are the lower and upper observation values of the studied output. N is the number of response variables and is the predicted value for the response.

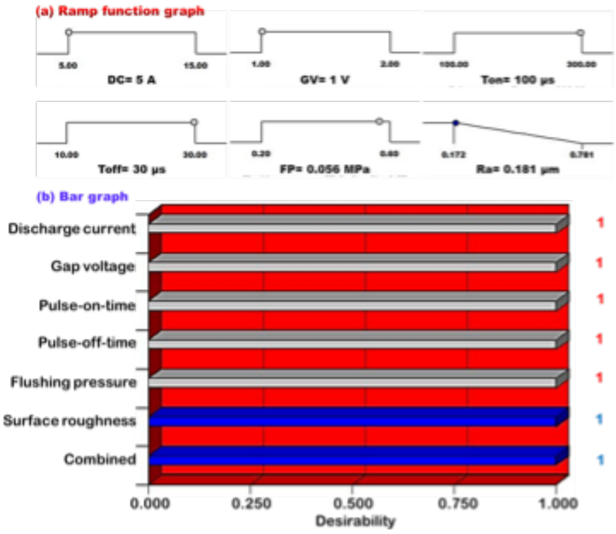

Figure 14. Optimization results using desirability function analysis.

With a set of thirty-one solutions, the optimum solution having the highest desirability value (i.e., close to 1) were sorted out on a ramp function graph, as shown in Fig. 14a. The optimal settings are indicated as points on each ramp graph, which results in maximum desirability values. A bar plot is shown in Fig. 14b that presents the individual desirability value of 1. As it is seen from Fig. 14, the optimum cutting solution is preferred at pulse-on-time of 100 µs, gap voltage of 1 V, pulse-off-time of 30 µs, discharge current of 4 A and flushing pressure of 0.056 MPa. The surface roughness of Ra value 0.181 µm was found at the optimum parametric machining conditions.

3.4. Cost analysis

In machining operations, the economic activity plays a vital role in improving production rate as well as product quality. Innovation, exploration, planning and the use of resources are still being attempted to ensure the machining process more effectively, efficiently, commercially sustainable and environmentally safe. This involves knowledge or consciousness of the factors which control or influence machining economy and how. All the aspects for achieving the specific production target and overall economy need to be considered while planning and executing the different operational stages right from product design to finishing of the product. The basic machining requirements – the machining process and system, tool material & geometry, process parameters – are to be appropriately selected and optimized so that the desired economy in terms of productivity, product quality, machining cost, profit or profitability is fulfilled. This requires knowledge of both theories of machining and optimization. For this reason, a cost analysis is executed at optimum parametric settings according to the desirability function approach of RSM in order to estimate the total cost per component. Table 6 shows a detailed economic analysis in EDM of Al-SiC MMC with brass electrode using bio-degradable eco-friendly vegetable oil. It is noted that the overall machining cost per component is low (Rs. 245.90; 2.95 €) and justifies considerable economic advantages to machining Al-SiC MMC as the production cost is reduced.

3.5. Sustainability assessment

Due to strict regulation of government policies and manufacturing constraints with regard to the state of affairs in cleaner production, sustainability assessment of every production methodology performs a key aspect prior to its actual practice in industry. Now-a-days, sustainable manufacturing is increasingly attracting attention in various indus-

Table 6. Machining economic assessment of Al-22%SiC MMC in EDM

Production costs and times	Al-22%SiC MMC
Tool electrode positioning time, (T_p)	1 min
Locating and clamping time of workpiece, (T_{clamp})	5 min
Machining time per hole drilling, (T_{edr})	15.5 min
Duration of procedure followed for electrode drawing-out, (T_d)	1 min
Overall machining time per hole, $(T_{ovl} = T_{clamp} + T_{edr} + T_p + T_d)$	22.5 min
Each electrode's cost, (C_{edr})	Rs. 20 (0.24 €)
Serviceable cost of machine, (C_m)	Rs. 8.33/min (0.1 €/min)
Operator rate, (C_{op})	Rs. 5.83/min (0.07 €/min)
Overall machining cost expenditure per hole, $C_{ovl} = (C_{edr}) + (T_{ovl} \times C_m) + ([T_{clamp} + T_{edr}] \times 1.1 \times C_{op})$	Rs. 245.90 (2.95 €)

tries as it minimizes or eliminates processing and production wastes using eco-efficient practice and new environmental technologies. Thus, all levels of manufacturing activities (product, process and system), promise a long-term benefit from the environmental, social and economic points of view, as they manufacture the products using non-polluting and natural resources conserving economically sound and safe processes.

EDM process approaches several economic, environmental, and social issues, particularly, poor MRR, high EWR & energy consumption, degraded surface characteristics, unsafe emissions around operator working area, danger of fire explosion and generation of hazardous waste and sludge (D'Urso *et al.*, 2018). EDM generally employs a dielectric fluid like deionized water or hydrocarbon oils. This oil contains aromatic, naphthenic and paraffinic compounds, which are considered as the major emission sources in EDM. During the spark erosion process, several toxic contents are formed, which are extremely efficient to penetrate the human body via the skin contact and inhalation. Long exposure to such harmful compounds will lead to cancer, respiratory diseases and dermatitis. In comparison to the transformer oil and kerosene, the implementation of the employment of bio-degradable vegetable oil, as a dielectric medium, has shown improved machining efficiency and a new solution for the enhancement of process sustainability. The functional competence of the vegetable oil as a potential replacement as a dielectric has been evaluated, showing to be safer, cleaner and greener solutions to enhance the sustainability of the EDM process.

With reference to the sustainability perspective, a new approach is assumed to propose an index, which can be applied in real practice for industrial decision making. This index would deal with the selection of the dielectric fluid in EDM process. In this context, a sustainability index (SI) was established as a tool that can be used in various technological contexts depending on the applied multicriteria logic employed. In this paper, an Indian currency-based sustainability index (SI) was expressed quantitatively to reflect the dielectric consumption usage and its environmental effect that results from the use of two different oils (kerosene and vegetable oil) in the EDM process. A high value of SI indicates poor sustainability. When the index has a low value, the process has a lesser impact and is thus more sustainable.

In order to formulate ***SI***, the parameters considered are as follows:

Dielectric consumption: The assessment of the dielectric impact is accomplished by considering the purchase price of both dielectrics, its filtration & disposal costs. The dielectric cost ($\boldsymbol{C_d}$), purchase cost of filter ($\boldsymbol{C_f}$), and dismantling cost of the dielectric ($\boldsymbol{C_s}$) are represented in Eqs. (4)-(6) and are calculated as follows (Pellegrini and Ravasio, 2019):

$$C_d = \frac{C_{ad}.V_d.t_e}{L_d} \tag{4}$$

$$C_f = \frac{C_{af}.t_e}{L_f} \tag{5}$$

$$C_s = \frac{C_s.V_d.t_e}{L_d} \tag{6}$$

where $\boldsymbol{C_{ad}}$ is the dielectric price per liter expressed in Rs./ltr., Vd is the volume of dielectric tank expresses in liters, $\boldsymbol{L_d}$ is the life of dielectric fluid in hours, $\boldsymbol{C_{af}}$ is the cost of a filter in ***Rs.*** and $\boldsymbol{L_f}$ is the life of unit filter in hours, $\boldsymbol{C_{as}}$ is the unitary dielectric dismantling cost per liter in Rs./ltr. and $\boldsymbol{t_e}$ is the erosion time in hours, which is defined as the time gap between the beginning and end of the machining cycle. As a result, this involves a time duration where the machine makes no attempt to erode (in particular, the time used for controlling the tool wear). Exclusively, the active time must be included but considering that the duration of the machining operation is more than the passive time, assuming that it is negligible and leads to an acceptable approximation.

The overall sustainability index due to dielectric consumption can be expressed as;

$$S_{dielectric} = C_d + C_f + C_s = \left(\frac{(C_{ad} + C_s)V_d}{L_d} + \frac{C_{af}}{L_f}\right)t_e \tag{7}$$

It is revealed that the overall influence of dielectric on sustainability is depending upon the machining duration and it is thus based on MRR directly. Table 7 reveals the coefficients' values employed in the Eqs. (4)-(7) for the calculation of sustainability index.

Table 7. Coefficients' values (the cost in € has been estimated and included in brackets as a more international reference).

Variables	Kerosene	Vegetable oil
V_d, ltr	400	400
C_{ad}, Rs./ltr (€/ltr)	55 (0.66)	90 (1.08)
C_{af}, Rs. (€)	3000 (35.96)	3000 (35.96)
L_d, hr	1000	1000
L_f, hr	1000	1000
C_s, Rs./ltr (€/ltr)	15 (0.18)	15 (0.18)

Environmental impact: Different multiple parameters were considered like fire hazard, toxic fumes development, operator's skin irritation, dust generation, re-use of dielectric, dielectric dismantling and its filters dismantling. For achieving the sustainability needs, an efficient decision-making approach called Pugh matrix (refer, Table 8) is proposed by assigning a weigh score to above stated environmental sustainability parameters (in the range of 0-2) based on its importance i.e., best-to-worst criterion (the score '2' indicates that the environmental impact is more severe). After considering these weights, the penalty coefficient K_i is calculated. K_i is the ratio between the sum of these evaluations and the maximum achievable points. Thereafter, the estimated value of K_i is substituted in Eq. (8) for the assessment of environmental sustainability.

Table 8. Score allocation to various environmental sustainability parameters in the Pugh matrix for estimation of the penalty coefficient.

	Kerosene	**Vegetable oil**
Filter dismantling	2	2
Fire hazard	2	0
Skin irritation	2	0
Fume production	2	2
Dielectric re-use	1	1
Dust generation	0	0
Dielectric dismantling	2	2
Toxic fumes	2	1
Total	13	8
Penalty coefficient, K_i	0.81	0.5

The environmental sustainability ($E_{nvironmental}$) is calculated by;

$$S_{Environmental} = (1 + K_i)\beta . t_e \tag{8}$$

where, β is an unitary coefficient expressed in Rs./hr. Finally, the overall sustainability index (***SI***) in rupees (Rs.) is determined by,

$$SI = S_{Dielectric} + S_{Environmental} \tag{9}$$

It is observed that the sustainability index established is influenced by the machining time. Figure 15 clearly shows the graphical variations in the sustainability index based on the above data with the use of different dielectrics. The result of vegetable oil outperformed that of the kerosene. In general, the use of kerosene oil as a dielectric in EDM is less sustainable compared to waste vegetable oil in all conditions. Besides, in various technical contexts such as µ-EDM or WEDM the proposed index may be applied. Such tool is a well adopted to propose alternative dielectrics which are not yet used in industrial practice. The index proposed for the sustainability assessment of the EDM process uses a strategy to enhance the knowledge in the selection of alternative dielectrics during the decision-making stage, unexploited in industrial application, and aiming at obtaining an environmental impact reduction. Exceptional dielectric fluids such as the vegetable oil have proven to be a true replacement to boost the sustainability and encouraged the implementation of a more realistic production approach for the EDM technology.

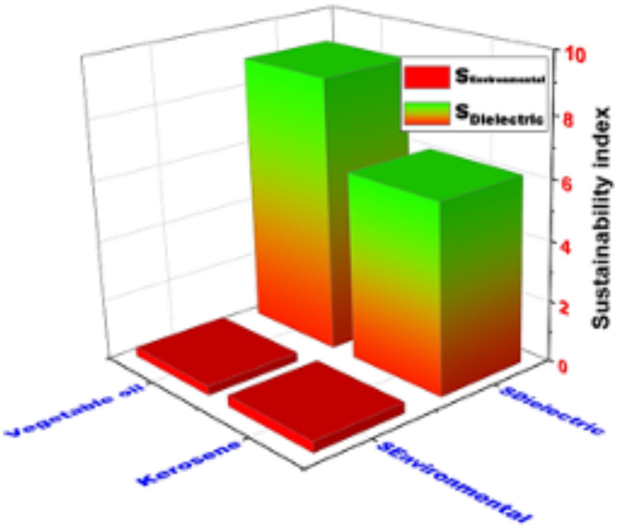

Figure 15. Sustainability index of electrical discharge machining when the dielectric changes from kerosene to vegetable oil.

4. CONCLUSIONS

With reference to the experimental findings and analysis of the results, modelling & optimization considerations, the economic analysis and the comparative sustainability assessment related to the EDM of Al-22%SiC MMC, the following outcomes are listed below:

- The contribution of spark discharge current was identified as the leading factor in surface quality degradation, which states the status of the poor machined surface with regard to globules of debris, crater marks, voids, uneven fusion structure, surface microcracks.
- Based on the statistical error assessment (correlation coefficient R^2-value, Anderson-Darling normality test, P & F values of ANOVA and predictability plot), the developed predictive model for surface roughness presented a high degree of accuracy and probabilistic validity.
- Using the desirability function analysis of RSM, the optimum cutting solution was pre-

ferred at pulse-on-time of 100 μs, gap voltage of 1 V, pulse-off-time of 30 μs, discharge current of 4 A and flushing pressure of 0.056 MPa. The estimated surface roughness of Ra value 0.181 μm and the calculated overall machining cost per part of Rs.245.9 (2.95 €) were found, which indicates that it is techno-economically viable.

- The index proposed for the sustainability assessment of EDM process used a strategy to enhance the knowledge in the selection of alternative dielectrics during the decision-making stage, unexploited in industrial application, and aiming at obtaining an environmental impact reduction. Exceptional dielectric fluids such as the vegetable oil have proven to be a true replacement to boost the sustainability and encouraged the implementation of a more realistic production approach for the EDM technology.
- The research outcomes along with proposed predictive design optimization will offer useful practicable information for difficult-to-machine Al-SiC MMC.

REFERENCES

Belloufi, A., Mezoudj, M., Abdelkrim, M., Rezgui, I., Chiba, E. (2020). Experimental and predictive study by multi-output fuzzy model of electrical discharge machining performances. *Int. J. Adv. Manuf. Technol.* 109, 2065-2093. https://doi.org/10.1007/s00170-020-05718-8.

Bharathi Raja, S., Srinivas Pramod, C.V., Vamshee Krishna, K., Ragunathan, A., Vinesh, S. (2013). Optimization of electrical discharge machining parameters on hardened die steel using Firefly Algorithm. *Eng. Comput.* 31(1), 1–9. https://doi.org/10.1007/s00366-013-0320-3.

Bharti, P.S., Maheshwari, S., Sharma, C. (2012). Multi-objective optimization of electric-discharge machining process using controlled elitist NSGA-II. *J. Mech. Sci. Technol.* 26 (6), 1875–1883. https://doi.org/10.1007/s12206-012-0411-x.

Cakir, M.V., Eyercioglu, O., Gov, K., Sahin, M., Cakir, S.H. (2013). Comparison of Soft Computing Techniques for Modelling of the EDM Performance Parameters. *Adv. Mech. Eng.* 5, 392531. https://doi.org/10.1155/2013/392531.

Chattopadhyay, K.D., Verma, S., Satsangi, P.S., Sharma, P.C. (2009). Development of empirical model for different process parameters during rotary electrical discharge machining of copper–steel (EN-8) system. *J. Mater. Process. Technol.* 209 (3), 1454–1465. https://doi.org/10.1016/j.jmatprotec.2008.03.068.

Chaudhury, P., Samantaray, S. (2021). Modelling and Optimization of Machining of SiC-CNT Conductive Ceramic Composite used for Micro and Nano Sensor by Electrical Discharge Machining. *J. Inst. Eng. India Ser. D*. https://doi.org/10.1007/s40033-021-00256-3.

Dash, L., Padhan, S., Das, S.R. (2020). Experimental investigations on surface integrity and chip morphology in hard tuning of AISI D3 steel under sustainable nanofluid-based minimum quantity lubrication. *J. Braz. Soc. Mech. Sci. Eng.* 42 (10), 500. https://doi.org/10.1007/s40430-020-02594-x.

D'Urso, G., Giardini, C., Ravasio, C. (2018). Effects of Electrode and Workpiece Materials on the Sustainability of Micro-EDM Drilling Process. *Int. J. Precis. Eng. Manuf.* 19 (11), 1727–1734. https://doi.org/10.1007/s12541-018-0200-2.

Ekmekci, B. (2007). Residual stresses and white layer in electric discharge machining (EDM). *Appl. Surf. Sci.* 253 (23), 9234–9240. https://doi.org/10.1016/j.apsusc.2007.05.078

Gao, Q., Zhang, Qh., Su, S., Zhang, J. (2008). Parameter optimization model in electrical discharge machining process. *J. Zhejiang Univ. Sci. A* 9 (1), 104–108. https://doi.org/10.1631/JZUS.A071242.

Garcia Rojas, E.E.G., Coimbra, J.S.R., Telis-Romero, J. (2013). Thermophysical Properties of Cotton, Canola, Sunflower and Soybean Oils as a Function of Temperature. *Int. J. Food Prop.* 16 (7), 1620–1629. https://doi.org/10.1080/10942912.2011.604889.

Gohil, V., Puri, Y. M. (2016). Statistical analysis of material removal rate and surface roughness in electrical discharge turning of titanium alloy (Ti-6Al-4V). *Proc. Inst. Mech. Eng. B J. Eng. Manuf.* 232 (9), 1603–1614. https://doi.org/10.1177/0954405416673104.

Gopalakannan, S., Senthilvelan, T. (2013). A parametric study of electrical discharge machining process parameters on machining of cast Al/B4C metal matrix nanocomposites. *Proc. Inst. Mech. Eng. B J. Eng. Manuf.* 227 (7), 993–1004. https://doi.org/10.1177/0954405413479505.

Hanif, M., Wasim, A., Shah, A.H., Noor, S., Sajid, M., Mujtaba, N. (2019). Optimization of process parameters using graphene-based dielectric in electric discharge machining of AISI D2 steel. *Int. J. Adv. Manuf. Technol.* 103, 3735–3749. https://doi.org/10.1007/s00170-019-03688-0.

Jagadish, Kumar, S. Soni, D.L. (2021). Performance Analysis and Optimization of Different Electrode Materials and Dielectric Fluids on Machining of High Carbon High Chromium Steel. In Electrical Discharge Machining. *Proc. Natl. Acad. Sci., India, Sect. A Phys. Sci.* https://doi.org/10.1007/s40010-020-00727-4.

Keskin, Y., Halkacı, H.S., Kizil, M. (2005). An experimental study for determination of the effects of machining parameters on surface roughness in electrical discharge machining (EDM). *Int. J. Adv. Manuf. Technol.* 28 (11-12), 1118–1121. https://doi.org/10.1007/s00170-004-2478-8.

Kumar, S., Batish, A., Singh, R., Singh, T.P. (2014). A hybrid Taguchi-artificial neural network approach to predict surface roughness during electric discharge machining of titanium alloys. *J. Mech. Sci.Technol.* 28 (7), 2831–2844.

Kumar, S., Dhingra, A.K., Kumar, S. (2017). Parametric optimization of powder mixed electrical discharge machining for nickel-based superalloy inconel-800 using response surface methodology. *Mech. Adv. Mater. Mod. Process.* 3 (1), 7. https://doi.org/10.1186/s40759-017-0022-4.

Kumar, A., Grover, N., Manna, A., Chohan J.S., Kumar, R., Singh, S., Prakash, C., Pruncu, C.I. (2020). Investigating the influence of WEDM process parameters in machining of hybrid aluminum composites. *Adv. Compos. Lett.* 29, 1-14. https://doi.org/10.1177/2633366X20963137.

Majumder, A. (2014). Comparative study of three evolutionary algorithms coupled with neural network model for optimization of electric discharge machining process parameters. *Proc. Inst. Mech. Eng. B J. Eng. Manuf.* 229 (9), 1504–1516. https://doi.org/10.1177/0954405414538960.

Marichamy, S., Saravanan, M., Ravichandran, M., Veerappan, G. (2016). Parametric optimization of electrical discharge machining process on α–β brass using grey relational analysis. *J. Mater. Res.* 31 (16), 2531–2537. https://doi.org/10.1557/jmr.2016.213.

Markopoulos, A.P., Manolakos, D.E., Vaxevanidis, N.M. (2008). Artificial neural network models for the prediction of surface roughness in electrical discharge machining. *J. Intell. Manuf.* 19 (3), 283–292. https://doi.org/10.1007/s10845-008-0081-9.

Mohan, B., Rajadurai, A., Satyanarayana, K.G. (2004). Electric discharge machining of Al–SiC metal matrix composites using rotary tube electrode. *J. Mater. Process. Technol.* 153-154, 978–985. https://doi.org/10.1016/j.jmatprotec.2004.04.347.

Mohanty, C.P., Mahapatra, S.S., Singh, M.R. (2014). A particle swarm approach for multi-objective optimization of electrical discharge machining process. *J. Intell. Manuf.* 27 (6), 1171–1190. https://doi.org/10.1007/s10845-014-0942-3.

Mohanty, C.P., Mahapatra, S.S., Singh, M.R. (2017). An intelligent approach to optimize the EDM process parameters using utility concept and QPSO algorithm. *Eng. Sci.*

Technol. Int. J. 20 (2), 552–562. https://doi.org/10.1016/j.jestch.2016.07.003.

Muthuramalingam, T., Mohan, B. (2013). Influence of Discharge Current Pulse on Machinability in Electrical Discharge Machining. *Mater. Manuf. Process.* 28 (4), 375–380. https://doi.org/10.1080/10426914.2012.746700.

Naik, S., Das, S.R., Dhupal, D. (2020). Experimental Investigation, Predictive Modeling, Parametric Optimization and Cost Analysis in Electrical Discharge Machining of Al-SiC Metal Matrix Composite. *Silicon* 13, 1017-1040. https://doi.org/10.1007/s12633-020-00482-6.

Pellegrini, G; Ravasio, C. (2019). Evaluation of the sustainability of the micro-electrical discharge milling process. *APEM* 14 (3), 343-354. https://doi.org/10.14743/apem2019.3.332.

Prabhu, S., Uma, M., Vinayagam, B.K. (2013). Electrical discharge machining parameters optimization using response surface methodology and fuzzy logic modeling. *J. Braz. Soc. Mech. Sci. Eng.* 36 (3), 637–652. https://doi.org/10.1007/s40430-013-0112-0.

Pradhan, M.K., Das, R., Biswas, C.K. (2009). Comparisons of neural network models onsurface roughness in electrical discharge machining. *Proc. Inst. Mech. Eng. B J. Eng. Manuf.* 223 (7), 801–808. https://doi.org/10.1243/09544054JEM1367.

Prakash, C., Kansal, H.K., Pabla, B.S., Puri, S. (2016). Multi-objective optimization of powder mixed electric discharge machining parameters for fabrication of biocompatible layer on β-Ti alloy using NSGA-II coupled with Taguchi based response surface methodology. *J. Mech. Sci. Technol.* 30 (9), 4195–4204. https://doi.org/10.1007/s12206-016-0831-0.

Puertas, I., Perez, C.J.L. (2003). Modelling the manufacturing parameters in electrical discharge machining of siliconized silicon carbide. *Proc. Inst. Mech. Eng. B J. Eng. Manuf.* 217 (6), 791–803. https://doi.org/10.1243/09544050360673170.

Rahul, Datta, S., Biswal, B.B., Mahapatra, S.S. (2017). A Novel Satisfaction Function and Distance-Based Approach for Machining Performance Optimization During Electro-Discharge Machining on Super Alloy Inconel 718. *Arab. J. Sci. Eng.* 42 (5), 1999–2020. https://doi.org/10.1007/s13369-017-2422-5.

Rahul, Datta, S., Biswal, B.B., Mahapatra, S.S. (2019). Machinability Analysis of Inconel 601, 625, 718 and 825 during Electro-Discharge Machining: On Evaluation of Optimal Parameters Setting. *Measurement* 137, 382-400. https://doi.org/10.1016/j.measurement.2019.01.065.

Ramesh, S., Jenarthanan, M.P. (2021). Optimizing the powder mixed EDM process of nickel based super alloy. *Proc. Inst. Mech. Eng. E J. Process. Mech. Eng.* 235 (4), 1092-1103. https://doi.org/10.1177/09544089211002782.

Raza, M.H., Wasim, A., Ali, M.A., Hussain, S., Jahanzaib, M. (2018). Investigating the effects of different electrodes on Al6061-SiC-7.5 wt% during electric discharge machining. *Int. J. Adv. Manuf. Technol.* 99 (9–12), 3017–3034. https://doi.org/10.1007/s00170-018-2694-2.

Reddy, V.V., Valli, P.M., Kumar, A., Reddy, C.S. (2014). Multi-objective optimization of electrical discharge machining of PH17-4 stainless steel with surfactant-mixed and graphite powder–mixed dielectric using Taguchi-data envelopment analysis–based ranking method. *Proc. Inst. Mech. Eng. B J. Eng. Manuf.* 229 (3), 487–494. https://doi.org/10.1177/0954405414530904,

Sahu, S.K., Jadam, T., Datta, S., Nandi, G. (2018). Effect of using SiC powder-added dielectric media during electro-discharge machining of Inconel 718 superalloys. *J. Braz. Soc. Mech. Sci. Eng.* 40 (7), 330. https://doi.org/10.1007/s40430-018-1257-7.

Sahu, S.K., Datta, S. (2019). Experimental studies on graphite powder-mixed electro-discharge machining of Inconel 718 super alloys: Comparison with conventional electro-discharge machining. *Proc. Inst. Mech. Eng. E J. Process. Mech. Eng.* 233 (2), 384-402. https://doi.org/10.1177/0954408918787104.

Sahu, A.K., Thomas, J., Mahapatra, S.S. (2020). An intelligent approach to optimize the electrical discharge machining of titanium alloy by simple optimization algorithm. *Proc. Inst. Mech. Eng. E J. Process. Mech. Eng.* 235 (2), 371-383. https://doi.org/10.1177/0954408920964685.

Selvarajan, L., Manohar, M., Udhaya kumar, A., Dhinakaran, P. (2017). Modelling and experimental investigation of process parameters in EDM of Si3N4-TiN composites using GRA-RSM. *J. Mech. Sci. Technol*. 31 (1), 111–122. https://doi.org/10.1007/s12206-016-1009-5.

Senthil Kumar, R., Suresh, P. (2019). Experimental study on electrical discharge machining of Inconel using RSM and NSGA optimization technique. *J. Braz. Soc. Mech. Sci. Eng.* 41, 35. https://doi.org/10.1007/s40430-018-1526-5.

Shabgard, M.R., Farahmand, M R., Ivanov, A. (2009). Mathematical modelling and comparative study of the machining characteristics in ultrasonic-assisted electrical discharge machining of cemented tungsten carbide (WC—10%Co). *Proc. Inst. Mech. Eng. B J. Eng. Manuf.* 223 (9), 1115–1126. https://doi.org/10.1243/09544054JEM1461.

Singh, S. (2012). Optimization of machining characteristics in electric discharge machining of 6061Al/Al_2O_3p/20P composites by grey relational analysis. *Int J. Adv. Manuf. Technol.* 63 (9-12), 1191–1202. https://doi.org/10.1007/s00170-012-3984-8.

Singh, B., Kumar, J., Kumar, S. (2015). Optimization and surface modification in electrical discharge machining of AA 6061/SiCp composite using Cu–W electrode. *Proc. Inst. Mech. Eng. Pt. L J.* 231 (3), 332–348. https://doi.org/10.1177/1464420715596544.

Singh, J., Sharma, R.K. (2017). Multi-objective optimization of green powder-mixed electrical discharge machining of tungsten carbide alloy. *Proc. Inst. Mech. Eng. Part C* 232 (16), 2774–2786. https://doi.org/10.1177/0954406217727306.

Singh, N.K., Kumar, S., Singh, Y., Sharma, V. (2019). Predictive analysis of surface finish in gas assisted electrical discharge machining using statistical and soft computing techniques. *Surf. Rev. Lett.* 27 (4), 1950126. https://doi.org/10.1142/s0218625x19501269.

Sivam, S.P., Michaelraj, A.L., Kumar, S.S., Prabhakaran, G., Dinakaran, D., Ilankumaran, V. (2013). Statistical multi-objective optimization of electrical discharge machining parameters in machining titanium grade 5 alloy using graphite electrode. *Proc. Inst. Mech. Eng. Part B* 228 (7), 736–743. https://doi.org/10.1177/0954405413511073.

Talla, G., Sahoo, D.K., Gangopadhyay, S., Biswas, C.K. (2015). Modeling and multi-objective optimization of powder mixed electric discharge machining process of aluminum/alumina metal matrix composite. *Int. J. Eng. Sci. Technol.* 18 (3), 369–373. https://doi.org/10.1016/j.jestch.2015.01.007.

Tang, L., Guo, Y.F. (2013). Electrical discharge precision machining parameters optimization investigation on S-03 special stainless steel. *Int. J. Adv. Manuf. Technol.* 70 (5-8), 1369–1376. https://doi.org/10.1007/s00170-013-5380-4.

Tang, L., Du, Y.T. (2014). Experimental study on green electrical discharge machining in tap water of Ti–6Al–4V and parameters optimization. *Int. J. Adv. Manuf. Technol.* 70 (1-4), 469–475. https://doi.org/10.1007/s00170-013-5274-5.

Tzeng, C.-J., Chen, R.-Y. (2013). Optimization of electric discharge machining process using the response surface methodology and genetic algorithm approach. *Int. J. Precis. Eng. Manuf.* 14 (5), 709–717. https://doi.org/10.1007/s12541-013-0095-x.

Uyyala, S.B., Kumar, A., Krishna, A.G. (2014). Performance analysis of electrical discharge machining parameters on RENE 80 nickel super alloy using statistical tools. *I.J.M.M.M.* 15 (3/4), 212-234. https://doi.org/10.1504/IJMMM.2014.060551.

Yadav, U.S., Yadava, V. (2014). Experimental modeling and multiobjective optimization of electrical discharge drilling of aerospace superalloy material. *Proc. Inst. Mech. Eng. Part B* 229 (10), 1764–1780. https://doi.org/10.1177/0954405414539299.

Yildiz, Y., Sundaram, M.M., Rajurkar, K.P. (2012). Statistical analysis and optimization study on the machinability of beryllium–copper alloy in electro discharge machining. *Proc. Inst. Mech. Eng. Part B* 226 (11), 1847–1861. https://doi.org/10.1177/0954405412457610.